

Collective dynamics of liquid aluminum probed by Inelastic X-ray Scattering.

T. Scopigno¹, U. Balucani², G. Ruocco³, F. Sette⁴

¹*Dipartimento di Fisica and INFM, Università di Trento, I-38100, Povo, Italy.*

²*Istituto di Elettronica Quantistica CNR, I-50127, Firenze, Italy.*

³*Dipartimento di Fisica and INFM, Università di L'Aquila, I-67100, L'Aquila, Italy.*

⁴*European Synchrotron Radiation Facility, B.P. 220 F-38043 Grenoble, Cedex France.*

(April 26, 2024)

An inelastic X-ray scattering experiment has been performed in liquid aluminum with the purpose of studying the collective excitations at wavevectors below the first sharp diffraction peak. The high instrumental resolution (up to 1.5 meV) allows an accurate investigation of the dynamical processes in this liquid metal on the basis of a generalized hydrodynamics framework. The outcoming results confirm the presence of a viscosity relaxation scenario ruled by a two timescale mechanism, as recently found in liquid lithium.

PACS numbers: 61.10.Eq, 67.40.Fd, 67.55.Jd, 63.50.+x

I. INTRODUCTION

In the last two decades, the dynamical properties of liquid metals have been widely investigated aiming at the comprehension of the role of the mechanisms underlying the atomic motions at the microscopic level. In particular, in the special case of alkali metals, it is known that well-defined oscillatory modes persist well outside the strict hydrodynamic region, down to wavelengths of a few inter-particle distances, making these systems an ideal workbench to test the different theoretical approaches developed so far for the microdynamics of the liquid state. By the experimental point of view, it is worth mentioning the pioneering inelastic neutron scattering (INS) experiment by Copley and Rowe [1] in liquid rubidium, while more recently a lot of experimental efforts in performing more and more accurate experiments have been done: INS investigations have been devoted to liquid cesium [2], sodium [3], lithium [4], potassium [5] and again rubidium [6]. Many numerical studies have been reported on the same systems, allowing to overcome experimental restriction such as the $(Q - E)$ accessible region when dealing with the collective properties (with the density fluctuation spectra), and the simultaneous presence of coherent and incoherent contribution in the INS signal, the paramount experimental technique in this field up to a few years ago. Moreover, numerical techniques allow to access a wider set of correlation function while the inelastic scattering experiment basically probe the density autocorrelation function.

On the theoretical side, thanks to the development of tools such as the memory function formalism, the relaxation concept, the kinetic theory, [7,8] a framework has been established in order to describe the behavior of the afore mentioned correlation functions. In this respect, among the most important task, there is the idea that the decay of the density autocorrelation function occurs over different time scales. In particular a first mecha-

nism is related to the coupling of the density and the temperature modes (thermal relaxation), while a second process involves the stress correlation function (viscosity relaxation). The latter mechanism proceeds through two different relaxation channels, active over different time scales: a first rapid decay, that has been ascribed to cage effects due to microscopic interaction of each atom and the cage of its neighboring atoms, followed by a slower process related to the long time rearrangements that drives the glass transition in those systems capable of supercooling. This structural relaxation process has been widely studied in the mode coupling formalism and recently remarkable efforts have been developed to set up self consistent approaches [9]. This theoretical framework has been tested on a number of numerical studies (see for example [10] and references therein). Indeed, the lineshape of the density correlation spectra extracted by INS (in those systems where it is allowed in the significant $(Q - E)$ region) did not allow to discriminate between different models including all the relevant relaxation processes at the microscopic level [2].

In the recent past, the development of new synchrotron radiation facilities opened the possibility of using X-rays to measure the $S(Q, \omega)$ (which is proportional to the scattered intensity) in the non-hydrodynamic region; in this case the photon speed is obviously much larger than the excitations velocity, and no kinematic restriction occurs. Moreover, in a monatomic system, the Inelastic X-ray Scattering (IXS) cross section is purely coherent and so it is directly associated with the dynamic structure factor.

Recently, an accurate IXS study on liquid lithium allowed to detect experimentally the presence of the relaxation scenario predicted by theory on this prototypical alkali metal [11]. In particular, the data have been analyzed within a generalized hydrodynamic approach [10,12] and, following a memory function formalism [7], it has been possible to detect the presence of two relax-

ation processes (additional to the thermal process resulting by the coupling of density and temperature variables) affecting the dynamics of the systems in the mesoscopic wavevector region [13]. This results, obtained with a phenomenological ansatz for the memory function originally proposed in a theoretical work by Levesque et al. [8], has been then deeply discussed pointing out the physical origin of such dynamical processes [14].

Although alkali metals are commonly referred to as the “paradigm of simple liquids”, other liquid metals always exhibit the characteristic structural and dynamical features that can be interpreted within the elementary approaches typically utilized when dealing with Lennard-Jones or alkali interatomic potentials [15,16]. A remarkable example is provided by liquid aluminum. Several theoretical [17] and numerical [18] works have been reported on this system. In fact, the basic common features of simple liquids, such as the presence of collective excitations in the coherent dynamic structure factor below Q_m and the positive dispersion of the sound speed associated to them have been extensively studied in this liquid. On the other hand, in this Q region no experimental data have been reported to provide a real test and/or comparison of collective dynamics. Indeed, in liquid Al, the high value of the isothermal sound speed $c_0 \sim 4700$ m/s prevents for kinematical reasons a study of the collective dynamics by inelastic neutron scattering (INS): below Q_m the available energy transfer is too limited to investigate the acoustic excitations properties. Accurate INS data have instead been reported at higher wavevectors where, however, the single particle response is mainly probed (see for example Ref. [19]).

In this work we present the study of the coherent dynamic structure factor, $S(Q, \omega)$, of liquid aluminum ($T = 1000$ K) by Inelastic X-ray Scattering, in a wavevector region, $0.05Q_m \leq Q \leq 0.5Q_m$, of crucial importance as far as the dynamical features of the collective motion are concerned.

II. THE EXPERIMENT

Our IXS experiment has been carried out at the high resolution beamline ID16 of the European Synchrotron Radiation Facility (Grenoble, F). The incident beam is obtained by a back-scattering monochromator operating at the $(hh\bar{h})$ silicon reflections, with $h=9, 11$. The scattered photons are collected by spherically bended Si crystal analyzers working at the same $(hh\bar{h})$ reflections. The total energy resolution function, measured from the elastic scattering by a Plexiglas sample, has a full width half maximum of 3 meV for $h=9$ and of 1.5 meV for $h=11$: this higher resolution configuration has been used at $Q = 1$ and 2 nm $^{-1}$, where the width of the spectral features starts to be comparable to the resolution width at $h=9$. The wavevector transferred in the scattering

process, $Q=2k_i \sin(\theta_s/2)$ (with k_i the wavevector of the incident photon and θ_s the scattering angle) is selected between 1 nm $^{-1}$ and 14 nm $^{-1}$ by rotating a 7 m long analyzer arm in the horizontal scattering plane. The total ($FWHM$) Q resolution has been set to 0.4 nm $^{-1}$. A five analyzers bench was used to collect simultaneously five different Q values, determined by a constant angular offset of 1.5° between neighboring analyzers. Energy scans have been performed by varying the temperature of the monochromator with respect to that of the analyzer crystals. Each scan took about 180 min, and each spectrum at a given Q was obtained from the average of 2 to 8 scans, depending on the values of h and of Q . The data have been normalized to the intensity of the incident beam. The liquid aluminum sample (0.999% purity) has been kept in an Al₂O₃ container with optically polished single crystal sapphire windows (0.25 mm thick). The sample length, which for an IXS scattering experiment is optimal if coincident with the absorption length, has been set to 1.0 mm in order to be nearly optimized for both $h = 9, 11$ energies (21747 and 17794 eV respectively). The cell was then host into a molybdenum oven in thermal contact with a tantalum foil heated by the dissipation of about 100 W of power. All the environment has been kept in 10 $^{-7}$ mbar dynamic vacuum.

The IXS spectra $I(Q, \omega)$, collected at fixed Q as functions of the exchanged energy, are reported in Fig. 1. As $Q_m = 25$ nm $^{-1}$, from the raw spectra we can observe the relevant region of dispersion of the acoustic mode. Initially, the frequency of the inelastic peaks increases linearly with Q . Despite an increase with Q of their width, the modes are recognizable even at the highest wavevectors explored in the experiment. As expected, the ratio between the energy loss/gain sides of the spectra is ruled out by the detailed balance condition. The quasi-elastic portion of the spectra, associated to some still unrelaxed damping mechanism, shows a linewidth that increases with Q , as the characteristic timescale of such process suddenly decreases at decreasing the dominant wavelength of the observed density fluctuation.

At the lower Q -values a non-negligible contribution coming from the empty container scattering is clearly visible (arrows in Fig. 1). This feature basically stems from the inelastic scattering of the sapphire windows. As the longitudinal phonon velocity in Al₂O₃ is more than 10000 m/s, this “spurious” contribution is beyond the energy region relevant for liquid Al and does not significantly affect the main spectral features of interest. However, for an accurate quantitative assessment of the spectral shape at the lower Q values, in the analysis we have excluded the undesired portions around the Al₂O₃ phonons by cutting off the two corresponding energy ranges (shadowed areas in Fig. 2).

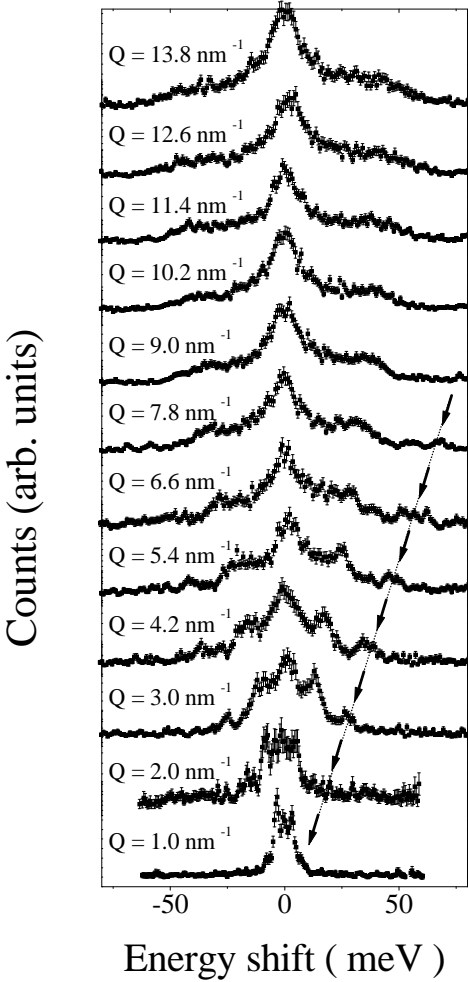


FIG. 1. IXS spectra of liquid aluminum at the indicated wavevectors. The instrumental resolution is $\Delta E = 1.5$ meV at $Q = 1$ and 2 nm $^{-1}$ and $\Delta E = 3.0$ meV elsewhere. The total integration time is about 500 s for each point.

III. DATA ANALYSIS

The spectra $S(Q, \omega)$ have been described within the framework of the generalized Langevin equation for the density correlator $\phi(Q, t) = \langle \rho_Q(t) \rho_{-Q}(0) \rangle / \langle |\rho_Q(t)|^2 \rangle$:

$$\ddot{\phi}(Q, t) + \omega_0^2(Q)\phi(Q, t) + \int_0^t M(Q, t - t') \dot{\phi}(Q, t') dt' = 0$$

where

$$\omega_0^2(Q) = [k_B T / m S(Q)] Q^2 = (c_0(Q) Q)^2, \quad (1)$$

In these equations, m is the atomic mass, $S(Q)$ the static structure factor, $c_0(Q)$ the Q -dependent isothermal sound velocity and $M(Q, t)$ the full memory function. Recalling that the Fourier transform of $\phi(Q, t)$

is $S(Q, \omega) / S(Q)$, and introducing the Fourier-Laplace transform of the memory function as $M(Q, \omega) = M''(Q, \omega) + iM'(Q, \omega)$, the previous expression becomes:

$$\frac{S(Q, \omega)}{S(Q)} = \frac{\pi^{-1} \omega_0^2(Q) M'(Q, \omega)}{[\omega^2 - \omega_0^2 + \omega M''(Q, \omega)]^2 + [\omega M'(Q, \omega)]^2} \quad (2)$$

All the details of the microscopic interactions are now embodied in the memory function $M(Q, t)$. For the latter, we have allowed a two-time relaxation mechanism of non-thermal contributions by assuming that

$$M(Q, t) = (\gamma - 1) \omega_0^2(Q) e^{-D_T Q^2 t} + \Delta^2(Q) [A(Q) e^{-t/\tau_\alpha(Q)} + (1 - A(Q)) e^{-t/\tau_\mu(Q)}] \quad (3)$$

where τ 's, Δ^2 and A are the timescales, the total viscous strength and the relative weight of the two processes respectively. In Eq. (3) the first term comes from the coupling between density and thermal fluctuations ($\gamma = C_P / C_V$ is the specific heats ratio and $D_T = \kappa / n C_V$ the thermal diffusivity), while the other two contributions describe the relaxation of purely viscous decay channels. As is well known, for the latter the familiar viscoelastic model assumes a single exponential decay. However, as already found in liquid lithium [13,14], this simple ansatz is not accurate enough to reproduce the details of the IXS spectra in liquid Al.

Before any discussion of the fitting procedure, we recall that the actual scattered intensity is proportional to the convolution between the experimental resolution function and the true (quantum mechanical) dynamic structure factor $S_q(Q, \omega)$, affected by the detailed balance condition. To account for the latter, we have used the following approximation

$$S_q(Q, \omega) = \beta \hbar \omega / (1 - e^{-\beta \hbar \omega}) S(Q, \omega) \quad (4)$$

which connects $S_q(Q, \omega)$ with its classical counterpart $S(Q, \omega)$.

Summing up, we used Eq.(2,3) as a model function. We modified it according to Eq.(4) and, finally, we folded it with the experimental resolution. The result has been utilized as fitting function $F(Q, \omega)$ for the scattered intensity $I(Q, \omega)$:

$$F(Q, \omega) = E(Q) \int R(\omega - \omega') S_q(Q, \omega') d\omega' \quad (5)$$

where the constant $E(Q)$ depends on each analyzer efficiency and on the atomic form factor. The parameters $S(Q)$ and $\omega_0^2(Q)$ are related by the Eq. (1), so that the most obvious procedure would be to put the data on an absolute scale estimating $S(Q)$ in a fitting-independent way and to fix $\omega_0^2(Q)$ accordingly. Consequently, *i*) the constant $E(Q)$ in Eq. (5) would be $E(Q) = 1$ *ii*) the only free fitting parameters would be the relaxation times and

strengths of the viscous channels (for the thermal quantities $D_T(Q)$ and $\gamma(Q)$ it has been utilized their $Q \rightarrow 0$ value). This method has been successfully applied in the lithium experiment, where the $S(Q)$ has been estimated from the raw spectra utilizing the first two sum rules corrected for finite resolution effects [14]. In the present case instead, due to the presence of empty cell contributions in the tails of the scattered intensity, an estimate of the spectral moment would be not reliable. For this reason we have chosen to leave $E(Q)$ and $\omega_0^2(Q)$ as free parameters. The best-fitted value of the latter quantity has been then used to calculate $S(Q)$, putting the data on absolute scale.

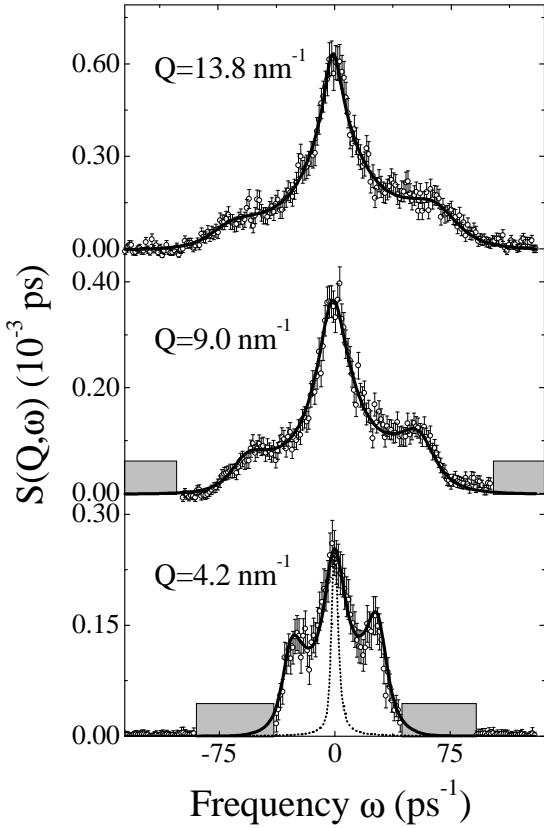


FIG. 2. Selected examples of the fitting procedure. Open circle with the error bars are the IXS data, the full lines are the best fit to the data. The shadow boxes indicate the energy windows that have been cut off in the fitting session. The resolution function is also reported (dotted line).

Some examples of the quality of the described fitting procedure are reported in Fig. 2, while the reliability of the normalization method is illustrated in Fig. 3, where the insert reports in a log scale the parameter $\omega_0^2(Q)$. The value of $S(Q)$ at small Q is seen to be in fair agreement with the thermodynamic value (arrow) [18].

In Fig. 4 the relative weight $A(Q) = \Delta_\alpha^2(Q)/(\Delta_\alpha^2(Q) + \Delta_\mu^2(Q))$ is shown. Compared to the liquid lithium, $A(Q)$ in liquid Al appears to have a faster decrease with the wavevector, indicating a somehow smaller role of slow features at finite wavevectors in this system.

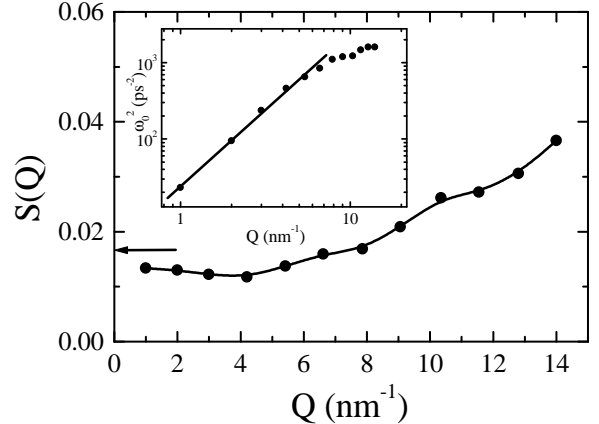


FIG. 3. Inset: $\omega_0^2(Q)$ as free fitting parameter. The full line is the expected power two behavior. Figure: Values of $S(Q)$ deduced by the previously determined $\omega_0^2(Q)$ as $S(Q) = KTQ^2/m\omega_0^2(Q)$. The arrow indicates the thermodynamic value of $S(0)$ by compressibility data.

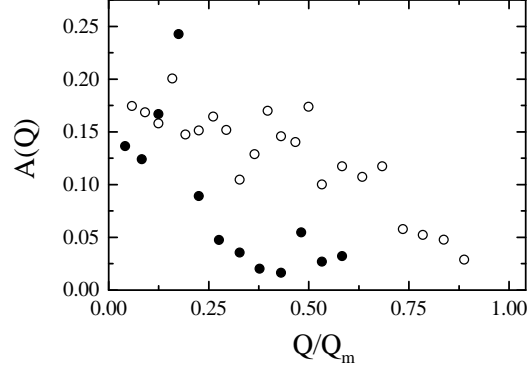


FIG. 4. Ratio, $A(Q)$, between the slow and the total relaxation strength. Full dots (\bullet) lithium, open dots (\circ) aluminum, both slightly above the melting point. In order to compare the two systems, the exchanged wavevector has been normalized to the static structure factor maximum.

In Fig. 5 we report for both mechanisms the relaxation times and, in the inset, the quantity $\omega_l(Q)\tau(Q)$, where $\omega_l(Q)$ is the maximum of the longitudinal current correlation spectra.

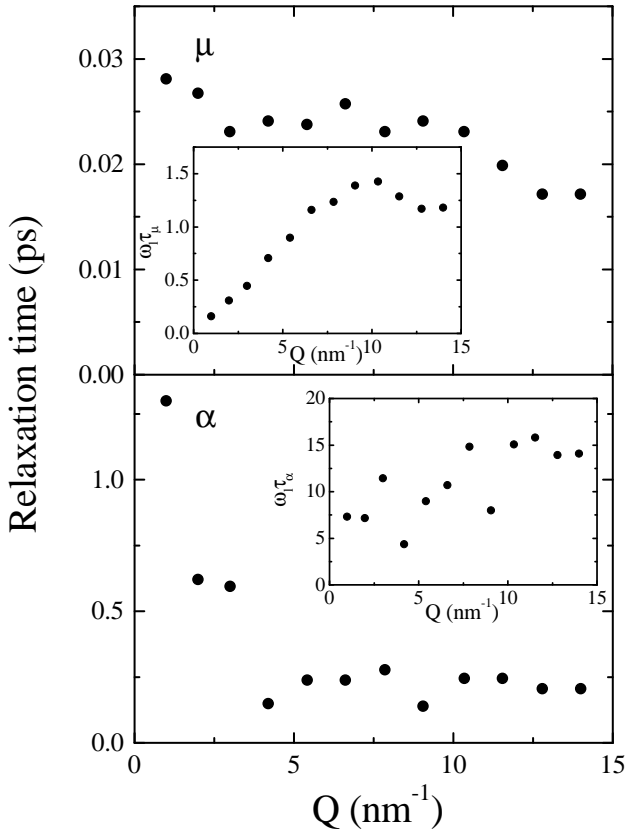


FIG. 5. Relaxation times and $\omega_l(Q)\tau(Q)$ values determined by the fitting

The characteristic time τ_μ of the microscopic process moderately decreases with Q , while the much longer τ_α is almost constant, except an abrupt initial decrease at very low Q which may be possibly due to finite resolution effects. From some algebraic manipulations of Eqs. (2,3), it is possible to infer the relations between the parameters ruling each mechanism and the main spectral features, i.e. the peak position and the width of the acoustic mode, as well as the intensity and the width of the central quasi-elastic contribution. From the inset of Fig. 5 it can be seen that for the slow process the condition $\omega_l(Q)\tau_\alpha(Q) > 1$ always holds, so that this mechanism contributes mostly to the elastic linewidth rather than to the acoustic mode broadening. On the other hand, the fast microscopic process is such that $\omega_l(Q)\tau_\mu(Q) \leq 1$ at low Q , so that in this region it contributes to the acoustic damping. However, at wavevectors $Q > 5 \text{ nm}^{-1}$, one reaches the crossover $\omega_l(Q)\tau_\mu(Q) \approx 1$, so that the fast mechanism drives an effective increase of the sound speed toward a limiting, solid-like, instantaneous response. As the weight of the fast process exceeds the one of the slow one (namely $A(Q) \ll 1$ in Eq. (3), cf. Fig. 4), the in-

crease of the sound speed basically stems only from the fast microscopic mechanism, which above the crossover threshold is also responsible for the broader tails of the quasi-elastic portion of the spectra ($\tau_\alpha \gg \tau_\mu$).

In Fig. 6 we report the *deconvoluted* spectra, i.e. the $S(Q, \omega)$ as obtained from the fitting procedure, together with the relative current correlation spectra $J(Q, \omega) = \omega^2/Q^2 S(Q, \omega)$. The latter quantity plays an important role in the description of the dynamical features of a systems because its maxima are related to $c_l = \omega_l/Q$, namely the apparent sound speed of the system.

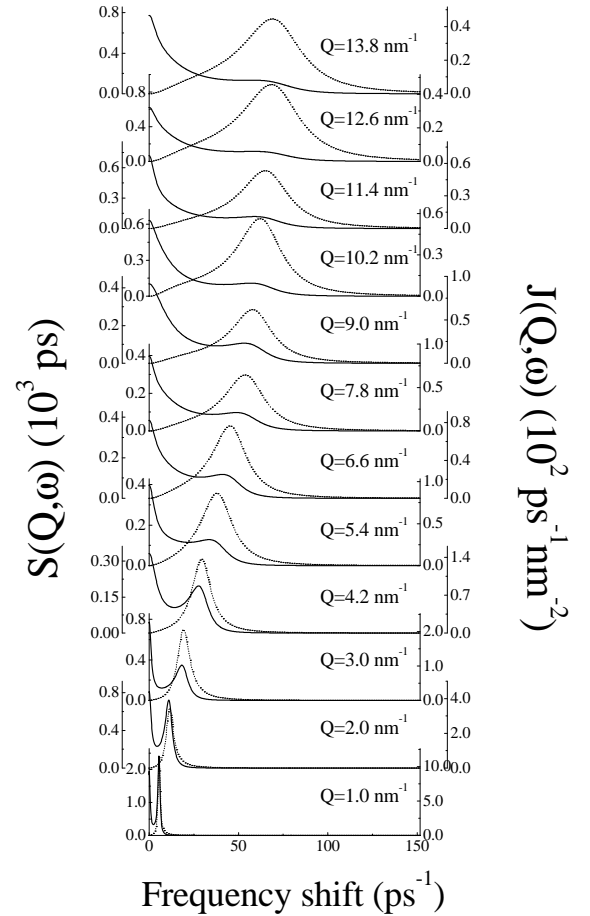


FIG. 6. Deconvoluted spectra of the density correlation function $S(Q, \omega)$ (left axis) and of the current correlation function $J(Q, \omega)$ (right axis) as obtained from the fit.

Finally, in Fig. 7, we compare the Q -dependent sound speed in liquid Al (calculated as the maximum of the fitting-deconvoluted longitudinal current correlation function $J(Q, \omega) = \omega^2/Q^2 S(Q, \omega)$) with the one previously determined in liquid lithium. Suitable reduced units (velocities normalized to their respective isothermal values, wavevectors measured in units Q_m) have been adopted.

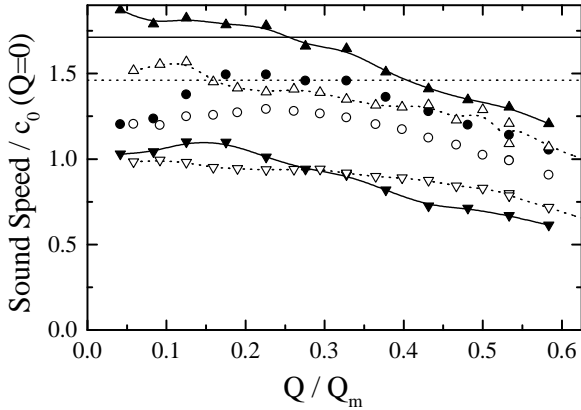


FIG. 7. Effective sound speed (dots) of aluminum (full symbols) vs lithium (open symbols). Data have been scaled by Q_m -the first sharp diffraction peak and $c_0(0)$ -the isothermal speed of sound in the hydrodynamic limit ($c_0^{Li} = 4450\text{m/s}$; $c_0^{Al} = 4700\text{m/s}$). $c_0(Q)$ is also reported ($-\nabla-$) together with the $c_\infty(Q)$ values determined by the fitting ($-\Delta-$) and by the pair distribution function and interatomic potential (lines). The lines connecting the symbols are guidelines for the eyes only.

Both systems are seen to exhibit a clear positive dispersion effect, i.e. an increase of the sound speed at increasing the exchanged wavevector. Such dispersion, in ordinary liquids, proceeds between the adiabatic ($Q \rightarrow 0$) limit, $c_s = \sqrt{\gamma}c_0$, and the unrelaxed, instantaneous value $c_\infty(Q) = \sqrt{\gamma\omega_0^2(Q) + \Delta^2(Q)}/Q$, where Δ^2 is the total strength of the non-thermal processes. In metallic liquids, instead, due to the high thermal conductivity, the condition $\omega_l(Q) < D_T Q^2$ holds for $Q \gtrsim 0.1\text{nm}^{-1}$, i.e., in the IXS Q -window ($Q > 1\text{nm}^{-1}$), no region exists where the three relaxation processes thermal, α , μ , are simultaneously unrelaxed. As a consequence, the lower and upper value of the sound speed are expected to be the isothermal $c_0(Q)$ (defined in Eq.(1)) and the partially unrelaxed $c'_\infty = \sqrt{\omega_0^2(Q) + \Delta_\alpha^2(Q) + \Delta_\mu^2(Q)}/Q$ [20].

To test the reliability of our model, we finally compared $c_\infty^{FIT}(Q)$ with the theoretical value $c_\infty^{TH}(0)$ deduced from the structure and interatomic potential data [17,21]. In both systems the fitted values of $c_\infty^{FIT}(Q \rightarrow 0)$ slightly exceed the data for $c_\infty^{TH}(0)$ reported in literature. A possible explanation of this inconsistency may be ascribed to the arbitrary choice of the memory function shape, that in principle can have more complicated features than the double exponential ansatz of Eq. (3). The major drawback of such an assumption is, indeed, the cusp at $t = 0$. It is reasonable to think that an exponential decay forced to represent a more complicated time dependence can give an accurate estimate as far as the τ is concerned, while at short times the lack of a zero second derivative inescapably leads to an overestimate of $M_L(Q, t = 0)$, the positive dispersion amplitude. A similar effect, i.e. the

overestimation of the $c_\infty(Q)$ deduced by the fit has been also observed in liquid lithium, where the same memory function has been adopted [14].

IV. CONCLUSION

In this work inelastic X-ray scattering technique has been utilized to study in detail the main features of the microscopic dynamics in liquid aluminum in the mesoscopic momentum region ($Q \approx 1 - 15\text{ nm}^{-1}$), i. e. the region where the collective properties are dominant. Aluminum is a system where the investigation of the dynamics using the well-established inelastic neutron scattering technique is not possible. The present IXS experiments allowed for the determination of the pattern of relaxation processes entering in the density-density memory function, and therefore affecting the spectral shape of the dynamic structure factor. Specifically, the high quality of the data allows to identify univocally the presence of three distinct relaxation processes. The first one - the usual thermal relaxation- is associated with the coupling between density and energy fluctuations. As in alkali metals, although its relevance is rather small, this process cannot be neglected; more interesting, it plays a role which is different with respect to the ordinary non-conducting liquids. Much more important is the unambiguous evidence of *two well separated timescales* in the decay of that part of the memory function which is associated to the generalized viscosity. In particular, the present experiment proves that the traditional description of the generalized viscosity by a single timescale (viscoelastic model) cannot account for the detailed shape of $S(Q, \omega)$, and that it only provides a qualitative description of the microscopic dynamics in liquid metals.

The presence of a two time-scales decay of the memory function poses a question of crucial importance: namely, their physical origin and, most important, of the fast one.

The slow process, making use of the terminology used to describe glass forming systems, is related to the α -relaxation which, in systems capable to sustain strong supercooling, is responsible for the liquid-glass transition. From a more canonical point of view, this process can be framed within kinetic theory in terms of "correlated collisions": in mode coupling approaches, the onset of these correlation effects is traced back to the coupling to slowly relaxing dynamical variables, and specifically in the liquid region, to long lasting density fluctuations. The quantitative description of this "slow" timescale requires a full evaluation of the mode-coupling contribution at different wavevectors which is beyond the aim of the present work.

As far as the fast process is concerned, the situation is more confused and its interpretation is still matter of debate. This is particularly annoying because -as shown in this paper for liquid aluminum and as demonstrated in

the case of liquid lithium- the fast process is indeed more relevant than the slow one: it largely controls both the sound velocity dispersion and attenuation in the mesoscopic Q region. Historically, within a generalized kinetic theory approach, the fast initial decay of the density fluctuation memory function, is traced back to *collisional events*, which are fast, short range and, more important, uncorrelated among each others. Within this scheme, the short timescale τ_μ turns out to be associated with the duration of a rapid structural rearrangement occurring over a spatial range $\cong 2\pi/Q_m$. Although this description of the fast process in term of uncorrelated interparticle collision is a possible way to qualitative account for the dynamical features at short times in liquids and dense systems, it seems to be unable to account for similar results obtained in glasses [21,22,24], where the *collective* aspect of the dynamics can not be neglected.

A possible, and different, approach to describe the initial fast decay of the memory function in dense fluids and liquids relies on the normal modes ("instantaneous" in normal liquids) analysis of the atomic dynamics [25], an approach that works correctly in the limiting case of "harmonic glasses". In this case one uses a framework (dynamical matrix, etc.) formally similar to the one customarily adopted for harmonic crystals; however, owing to the lack of translational symmetry of the system, it turns out [22] that the eigenstates cannot anymore be represented by plane waves (PW) even at relatively small wavevectors [26]. A scattering experiment, where Q is fixed, is equivalent -via the fluctuation-dissipation relation- to a response experiment, where one study the time evolution of the system after a *sinusoidal* perturbation (with period $2\pi/Q$) is applied to the system itself. In the case of measuring the $S(Q, \omega)$, the applied perturbation is a density fluctuation. As the PW are not eigenstate of the disordered systems, the initial perturbation can be projected along different eigenmodes, each one evolving in time with its own frequency. As a consequence of this frequency spread the energy initially stored in the PW *relax* towards other PW's with different Q values. This process is exactly what one expect in presence of a relaxation process, and its characteristic time is determined by the projection of the system eigenmodes on the PW basis (Fourier transform of the eigenvectors). We deal, therefore, with a mechanism whose ultimate origin is the topological disorder, and not a truly dynamical event. Ordinary liquids (such as the one considered here) are certainly "disordered systems" and at the high frequency considered here ($\omega\tau_\alpha \gg 1$), they can be considered as "frozen"; therefore the description used for glasses can be applied as well. Obviously, the "harmonic approximation" and the residual effect of the finite value of $\omega\tau$ prevent the "quantitative" application of the previously described formalism to the case of normal liquids. However we expect that -on a qualitative ground- the fast relaxation process in liquids can be described in

term of "high frequency vibrations" (that are a strongly correlated atomic motion), and this point of view appears to be in contrast with the (uncorrelated) binary collision based description.

At the present stage the experimental data cannot support either interpretation. However, the possibility that the phenomenology reported here for a simple liquid can be understood within the same mental framework developed for more complex liquids and glasses, is certainly appealing.

- [1] J. R. D. Copley and M. Rowe, Phys. Rev. A, **9**, 1656 (1974).
- [2] T. Bodensteiner, Chr. Morkel, W. Gläser and B. Dorner, Phys. Rev. A, **45**, 5709 (1992).
- [3] C. Morkel and W. Glaser, Phys. Rev. A **33**, 3383 (1986); A. Stangl, C. Morkel, U. Balucani and A. Torcini, J. Non-Cryst. Solids **205-207**, 402 (1996).
- [4] P. Verkerk, P. H. K. De Jong, M. Arai, S. M. Bennington, W. S. Howells and A. D. Taylor, Physica B **180 & 181**, 834 (1992).
- [5] A. G. Novikov, V. V. Savostin, A. L. Shimkevich, R. M. Yulmetyev and T. R. Yulmetyev, Physica B **228**, 312 (1996).
- [6] P. Chieux, J. Dupuy-Philon, J. F. Jal and J. B. Suck, J. Non Cryst. Solids **205-207**, 370 (1996).
- [7] H. Mori, Prog. Theor. Phys., **33**, 423, (1965).
- [8] D. Levesque, J. Verlet and J. Kurkijarvi, Phys. Rev. A **7**, 1690 (1973).
- [9] J. Casas, D. J. Gonzales and L. E. Gonzales, Phys. Rev. B **60**, 10094 (1999); J. Casas, D. J. Gonzales, L. E. Gonzales and M. Silbert, preprint of LAM 10, Dortmund (1998).
- [10] U. Balucani and M. Zoppi, Dynamics of the Liquid State (Clarendon Press, Oxford, 1994).
- [11] T. Scopigno, U. Balucani, A. Cunsolo, G. Ruocco, F. Sette, R. Verbeni, Europhys. Lett. **50**, 189 (2000); cond-mat/9911021.
- [12] J.P. Boon and S. Yip, Molecular Hydrodynamics (McGraw-Hill, New York, 1980).
- [13] T. Scopigno, U. Balucani, G. Ruocco, F. Sette, accepted by Phys. Rev. Lett. cond-mat/0009145
- [14] T. Scopigno, U. Balucani, G. Ruocco and F. Sette, Journal of Physics **12**, 8009 (2000). cond-mat/0001190.
- [15] M.M.G. Alemany, J. Casas, C. Rey, L.E. Gonzales, and L.J. Gallego, Phys. Rev. E **56**, 6818 (1997).
- [16] W. Gudowski, M. Dzugutov, and K.E. Larsson, Phys. Rev. E **47**, 1693 (1993).
- [17] T. Gaskell, J. Phys. F **16**, 381 (1986) and Phys. Chem. Liq. **17**, 11 (1987).
- [18] I. Ebbsjo, T. Kinnel and I. Waller, J. Phys. C: Solid State Physics, **13**, 1865 (1980).
- [19] O.J. Eder, B. Kunsch, J.B. Suck and M. Suda, Journal de Physique, 41, C8-226 (1980).
- [20] By a numerical point of view, the difference between

$c_\infty(Q)$ and $c'_\infty(Q)$ is of the order of $\sqrt{\gamma}$ (3%), namely, within the statistical errors of the fitting procedure. It is worth to point out how the thermal process, contrarily to what happens in ordinary liquids, gives also a non-viscous damping $\delta\omega = (\gamma - 1) c_0^2(Q)/D_T$, responsible for an additional Brillouin linewidth particularly important at the lower Q 's of our experiment.

- [21] T.Scopigno et al., in preparation.
- [22] G. Ruocco, F. Sette, R. Di Leonardo, G. Monaco, M. Sampoli, T. Scopigno and G. Viliani, Phys. Rev. Lett. **84**, 5788 (2000).
- [23] I. M. de Schepper and E. G. D. Cohen, J. Stat. Phys. **27**, 223 (1982).
- [24] W. Gotze and M.R. Mayr, Phys. Rev. E **61**, 587 (2000).
- [25] G. Seeley and T. Keyes, J. Chem. Phys. **91**, 5581 (1989).
- [26] V. Mazzacurati, G. Ruocco and M. Sampoli, Europhys. Lett. **34**, 681 (1996).